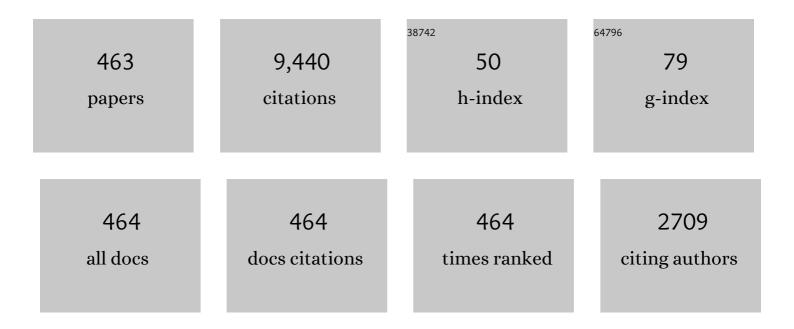
List of Publications by Year in descending order

Source: https://exaly.com/author-pdf/4351311/publications.pdf Version: 2024-02-01



MENCOAO XINC

#	Article	IF	CITATIONS
1	SAR Ground Maneuvering Targets Imaging and Motion Parameters Estimation Based on the Adaptive Polynomial Fourier Transform. IEEE Geoscience and Remote Sensing Letters, 2022, 19, 1-5.	3.1	2
2	Modified ERMA With Generalized Resampling for Maneuvering Highly Squinted TOPS SAR. IEEE Geoscience and Remote Sensing Letters, 2022, 19, 1-5.	3.1	3
3	First Demonstration of Using Signal Processing Approach to Suppress Signal Ringing in Impulse UWB Through-Wall Radar. IEEE Geoscience and Remote Sensing Letters, 2022, 19, 1-5.	3.1	2
4	Deep Mutual GAN for Life-Detection Radar Super Resolution. IEEE Geoscience and Remote Sensing Letters, 2022, 19, 1-5.	3.1	5
5	A Postmatched-Filtering Image-Domain Subspace Method for Channel Mismatch Estimation of Multiple Azimuth Channels SAR. IEEE Transactions on Geoscience and Remote Sensing, 2022, 60, 1-14.	6.3	4
6	Joint Estimation of Satellite Attitude and Size Based on ISAR Image Interpretation and Parametric Optimization. IEEE Transactions on Geoscience and Remote Sensing, 2022, 60, 1-17.	6.3	7
7	Focusing Translational-Variant Bistatic Forward- Looking SAR Data Using the Modified Omega-K Algorithm. IEEE Transactions on Geoscience and Remote Sensing, 2022, 60, 1-16.	6.3	5
8	Oriented Gaussian Function-Based Box Boundary-Aware Vectors for Oriented Ship Detection in Multiresolution SAR Imagery. IEEE Transactions on Geoscience and Remote Sensing, 2022, 60, 1-15.	6.3	15
9	Ultrahigh-Resolution Autofocusing for Squint Airborne SAR Based on Cascaded MD-PGA. IEEE Geoscience and Remote Sensing Letters, 2022, 19, 1-5.	3.1	6
10	Moving Target Radial Velocity Estimation Method for HRWS SAR System Based on Subspace Projection. IEEE Geoscience and Remote Sensing Letters, 2022, 19, 1-5.	3.1	4
11	An Improved SRGAN Based Ambiguity Suppression Algorithm for SAR Ship Target Contrast Enhancement. IEEE Geoscience and Remote Sensing Letters, 2022, 19, 1-5.	3.1	7
12	Spaceborne Synthetic Aperture Radar Imaging Algorithms: An overview. IEEE Geoscience and Remote Sensing Magazine, 2022, 10, 161-184.	9.6	29
13	Multiple Statistics Contributing to Few-Sample Deep Learning for Subtle Trace Detection in High-Resolution SAR Images. IEEE Transactions on Geoscience and Remote Sensing, 2022, 60, 1-14.	6.3	3
14	2-D Frequency Autofocus for Squint Spotlight SAR Imaging With Extended Omega-K. IEEE Transactions on Geoscience and Remote Sensing, 2022, 60, 1-12.	6.3	11
15	Polarization Image Demosaicking via Nonlocal Sparse Tensor Factorization. IEEE Transactions on Geoscience and Remote Sensing, 2022, 60, 1-10.	6.3	5
16	Integrating the Reconstructed Scattering Center Feature Maps With Deep CNN Feature Maps for Automatic SAR Target Recognition. IEEE Geoscience and Remote Sensing Letters, 2022, 19, 1-5.	3.1	8
17	AIS Data Aided Rayleigh CFAR Ship Detection Algorithm of Multiple-Target Environment in SAR Images. IEEE Transactions on Aerospace and Electronic Systems, 2022, 58, 1266-1282.	4.7	11
18	CANet: An Unsupervised Deep Convolutional Neural Network for Efficient Cluster-Analysis-Based Multibaseline InSAR Phase Unwrapping. IEEE Transactions on Geoscience and Remote Sensing, 2022, 60, 1-15.	6.3	18

#	Article	IF	CITATIONS
19	EFTL: Complex Convolutional Networks With Electromagnetic Feature Transfer Learning for SAR Target Recognition. IEEE Transactions on Geoscience and Remote Sensing, 2022, 60, 1-11.	6.3	17
20	Azimuth Variant Motion Error Compensation Algorithm for Airborne SAR Imaging Based on Doppler Adjustment. IEEE Geoscience and Remote Sensing Letters, 2022, 19, 1-5.	3.1	3
21	A Real-Time Unified Focusing Algorithm (RT-UFA) for Multi-Mode SAR via Azimuth Sub-Aperture Complex-Valued Image Combining and Scaling. IEEE Transactions on Geoscience and Remote Sensing, 2022, 60, 1-17.	6.3	5
22	SAR Target Classification Using the Multikernel-Size Feature Fusion-Based Convolutional Neural Network. IEEE Transactions on Geoscience and Remote Sensing, 2022, 60, 1-13.	6.3	42
23	Efficient Fast Time-Domain Processing Framework for Airborne Bistatic SAR Continuous Imaging Integrated With Data-Driven Motion Compensation. IEEE Transactions on Geoscience and Remote Sensing, 2022, 60, 1-15.	6.3	5
24	Structure-Awareness SAR Imagery by Exploiting Structure Tensor TV Regularization Under Multitask Learning Framework. IEEE Transactions on Geoscience and Remote Sensing, 2022, 60, 1-15.	6.3	3
25	An Effective Clutter Suppression Approach Based on Null-Space Technique for the Space-Borne Multichannel in Azimuth High-Resolution and Wide-Swath SAR System. IEEE Transactions on Geoscience and Remote Sensing, 2022, 60, 1-28.	6.3	1
26	Deep Learning-Based Branch-Cut Method for InSAR Two-Dimensional Phase Unwrapping. IEEE Transactions on Geoscience and Remote Sensing, 2022, 60, 1-15.	6.3	25
27	Motion Compensation/Autofocus in Airborne Synthetic Aperture Radar: A Review. IEEE Geoscience and Remote Sensing Magazine, 2022, 10, 185-206.	9.6	81
28	A Robust Image-Domain Subspace-Based Channel Error Calibration and Postimaging Reconstruction Algorithm for Multiple Azimuth Channels SAR. IEEE Transactions on Geoscience and Remote Sensing, 2022, 60, 1-18.	6.3	4
29	High-Speed Maneuvering Platform SAR Imaging With Optimal Beam Steering Control. IEEE Transactions on Geoscience and Remote Sensing, 2022, 60, 1-12.	6.3	3
30	Efficiency and Robustness Improvement of Airborne SAR Motion Compensation With High Resolution and Wide Swath. IEEE Geoscience and Remote Sensing Letters, 2022, 19, 1-5.	3.1	13
31	A Fine PolSAR Terrain Classification Algorithm Using the Texture Feature Fusion-Based Improved Convolutional Autoencoder. IEEE Transactions on Geoscience and Remote Sensing, 2022, 60, 1-14.	6.3	10
32	Joint Translational Motion Compensation Method for ISAR Imagery Under Low SNR Condition Using Dynamic Image Sharpness Metric Optimization. IEEE Transactions on Geoscience and Remote Sensing, 2022, 60, 1-15.	6.3	8
33	Radar Deception Jamming Recognition Based on Weighted Ensemble CNN With Transfer Learning. IEEE Transactions on Geoscience and Remote Sensing, 2022, 60, 1-11.	6.3	29
34	A Fast Cartesian Back-Projection Algorithm Based on Ground Surface Grid for GEO SAR Focusing. IEEE Transactions on Geoscience and Remote Sensing, 2022, 60, 1-14.	6.3	8
35	An Efficient Image Reconstruction Algorithm for Maneuvering Platform SAR Integrated With Elevation Information in Hybrid Coordinate System. IEEE Geoscience and Remote Sensing Letters, 2022, 19, 1-5.	3.1	0
36	Ship Focusing and Positioning Based on 2-D Ambiguity Resolving for Single-Channel SAR Mounted on High-Speed Maneuvering Platforms With Small Aperture. IEEE Transactions on Geoscience and Remote Sensing, 2022, 60, 1-13.	6.3	1

#	Article	IF	CITATIONS
37	PU-GAN: A One-Step 2-D InSAR Phase Unwrapping Based on Conditional Generative Adversarial Network. IEEE Transactions on Geoscience and Remote Sensing, 2022, 60, 1-10.	6.3	23
38	Super-Resolution Range and Velocity Estimations for SFA-OFDM Radar. Remote Sensing, 2022, 14, 278.	4.0	10
39	SAR Target Detection Based on Improved SSD with Saliency Map and Residual Network. Remote Sensing, 2022, 14, 180.	4.0	3
40	High-Resolution and Wide-Swath Imaging Based on Multifrequency Pulse Diversity and DPCA Technique. IEEE Geoscience and Remote Sensing Letters, 2022, 19, 1-5.	3.1	2
41	A Low Sidelobe Deceptive Jamming Suppression Beamforming Method With a Frequency Diverse Array. IEEE Transactions on Antennas and Propagation, 2022, 70, 4884-4889.	5.1	17
42	Comparative Study of DEM Reconstruction Accuracy Between Single- and Multibaseline InSAR Phase Unwrapping. IEEE Transactions on Geoscience and Remote Sensing, 2022, 60, 1-11.	6.3	8
43	High-Resolution Real-Time Imaging Processing for Spaceborne Spotlight SAR With Curved Orbit via Subaperture Coherent Superposition in Image Domain. IEEE Journal of Selected Topics in Applied Earth Observations and Remote Sensing, 2022, 15, 1992-2003.	4.9	9
44	Superâ€resolution forwardâ€looking imaging method for manoeuvering platform with optimised dictionary and extended sparsity adaptive matching pursuit. IET Radar, Sonar and Navigation, 2022, 16, 912-923.	1.8	4
45	Performance Improvement for SAR Tomography Based on Local Plane Model. IEEE Journal of Selected Topics in Applied Earth Observations and Remote Sensing, 2022, 15, 2298-2310.	4.9	8
46	A Novel CFFBP Algorithm With Noninterpolation Image Merging for Bistatic Forward-Looking SAR Focusing. IEEE Transactions on Geoscience and Remote Sensing, 2022, 60, 1-16.	6.3	5
47	Joint Estimation of Absolute Attitude and Size for Satellite Targets Based on Multi-Feature Fusion of Single ISAR Image. IEEE Transactions on Geoscience and Remote Sensing, 2022, 60, 1-20.	6.3	6
48	Varying Amplitude Vibration Phase Suppression Algorithm in ISAL Imaging. Remote Sensing, 2022, 14, 1122.	4.0	2
49	Range and Doppler reconstruction for sparse frequency agile linear frequency modulationâ€orthogonal frequency division multiplexing radar. IET Radar, Sonar and Navigation, 2022, 16, 1014-1025.	1.8	5
50	CRTransSar: A Visual Transformer Based on Contextual Joint Representation Learning for SAR Ship Detection. Remote Sensing, 2022, 14, 1488.	4.0	59
51	Number of targets detection method with FCMâ€based granulation–degranulation mechanism. Electronics Letters, 2022, 58, 445-447.	1.0	1
52	A Lightweight Position-Enhanced Anchor-Free Algorithm for SAR Ship Detection. Remote Sensing, 2022, 14, 1908.	4.0	26
53	Time-Domain Autofocus for Ultrahigh Resolution SAR Based on Azimuth Scaling Transformation. IEEE Transactions on Geoscience and Remote Sensing, 2022, 60, 1-12.	6.3	8
54	Noise Robust High-Speed Motion Compensation for ISAR Imaging Based on Parametric Minimum Entropy Optimization. Remote Sensing, 2022, 14, 2178.	4.0	4

#	Article	IF	CITATIONS
55	A heterogeneous double ensemble algorithm for soybean planting area extraction in Google Earth Engine. Computers and Electronics in Agriculture, 2022, 197, 106955.	7.7	6
56	Deep Ensemble CNN Method Based on Sample Expansion for Hyperspectral Image Classification. IEEE Transactions on Geoscience and Remote Sensing, 2022, 60, 1-15.	6.3	8
57	Attributed Scattering Center Extraction Method for Microwave Photonic Signals Using DSM-PMM-Regularized Optimization. IEEE Transactions on Geoscience and Remote Sensing, 2022, 60, 1-16.	6.3	3
58	Coherent Integration for Maneuvering Target Detection at Low SNR Based on Radon-General Linear Chirplet Transform. IEEE Geoscience and Remote Sensing Letters, 2022, 19, 1-5.	3.1	4
59	A High-Resolution and High-Precision Passive Positioning System Based on Synthetic Aperture Technique. IEEE Transactions on Geoscience and Remote Sensing, 2022, 60, 1-13.	6.3	6
60	Integration of Rotation Estimation and High-Order Compensation for Ultrahigh-Resolution Microwave Photonic ISAR Imagery. IEEE Transactions on Geoscience and Remote Sensing, 2021, 59, 2095-2115.	6.3	25
61	FEC: A Feature Fusion Framework for SAR Target Recognition Based on Electromagnetic Scattering Features and Deep CNN Features. IEEE Transactions on Geoscience and Remote Sensing, 2021, 59, 2174-2187.	6.3	81
62	Data-Driven Motion Compensation for Airborne Bistatic SAR Imagery Under Fast Factorized Back Projection Framework. IEEE Journal of Selected Topics in Applied Earth Observations and Remote Sensing, 2021, 14, 1728-1740.	4.9	11
63	Sub-aperture phase error stitching for full aperture airborne SAL data processing method based on azimuth deramp. Optics and Laser Technology, 2021, 136, 106708.	4.6	2
64	SVD-Based Ambiguity Function Analysis for Nonlinear Trajectory SAR. IEEE Transactions on Geoscience and Remote Sensing, 2021, 59, 3072-3087.	6.3	19
65	Ground Moving Target Indication for the Geosynchronous-Low Earth Orbit Bistatic Multichannel SAR System. IEEE Journal of Selected Topics in Applied Earth Observations and Remote Sensing, 2021, 14, 5072-5090.	4.9	12
66	Enhanced-Random-Feature-Subspace-Based Ensemble CNN for the Imbalanced Hyperspectral Image Classification. IEEE Journal of Selected Topics in Applied Earth Observations and Remote Sensing, 2021, 14, 3988-3999.	4.9	31
67	Joint Multitarget Detection and Tracking in Multipath Environment Using Expectation Maximization Algorithm. IEEE Journal of Selected Topics in Applied Earth Observations and Remote Sensing, 2021, 14, 10336-10347.	4.9	1
68	A Novel Two-Step Scheme Based on Joint GO-DPCA and Local STAP in Image Domain for Multichannel SAR-GMTI. IEEE Journal of Selected Topics in Applied Earth Observations and Remote Sensing, 2021, 14, 8259-8272.	4.9	7
69	ISAR Imaging Motion Compensation in Low SNR Environments Using Phase Gradient and Filtering Techniques. IEEE Transactions on Aerospace and Electronic Systems, 2021, 57, 4296-4312.	4.7	3
70	A Pixel Cluster CNN and Spectral-Spatial Fusion Algorithm for Hyperspectral Image Classification With Small-Size Training Samples. IEEE Journal of Selected Topics in Applied Earth Observations and Remote Sensing, 2021, 14, 4101-4114.	4.9	25
71	Processing of Bistatic SAR Data With Nonlinear Trajectory Using a Controlled-SVD Algorithm. IEEE Journal of Selected Topics in Applied Earth Observations and Remote Sensing, 2021, 14, 5750-5759.	4.9	22
72	Learning an SAR Image Despeckling Model Via Weighted Sparse Representation. IEEE Journal of Selected Topics in Applied Earth Observations and Remote Sensing, 2021, 14, 7148-7158.	4.9	11

#	Article	IF	CITATIONS
73	Water Body Detection in High-Resolution SAR Images With Cascaded Fully-Convolutional Network and Variable Focal Loss. IEEE Transactions on Geoscience and Remote Sensing, 2021, 59, 316-332.	6.3	36
74	Ultra-High Resolution Imaging Method for Distributed Small Satellite Spotlight MIMO-SAR Based on Sub-Aperture Image Fusion. Sensors, 2021, 21, 1609.	3.8	6
75	Time-Frequency Reversion-Based Spectrum Analysis Method and Its Applications in Radar Imaging. Remote Sensing, 2021, 13, 600.	4.0	4
76	Realizing Target Detection in SAR Images Based on Multiscale Superpixel Fusion. Sensors, 2021, 21, 1643.	3.8	9
77	Relative Total Variation Structure Analysis-Based Fusion Method for Hyperspectral and LiDAR Data Classification. Remote Sensing, 2021, 13, 1143.	4.0	5
78	Baseline Design for Multibaseline InSAR System: A Review. IEEE Journal on Miniaturization for Air and Space Systems, 2021, 2, 17-24.	2.7	19
79	Processing Missile-Borne SAR Data by Using Cartesian Factorized Back Projection Algorithm Integrated with Data-Driven Motion Compensation. Remote Sensing, 2021, 13, 1462.	4.0	3
80	Toward More Robust and Real-Time Unmanned Aerial Vehicle Detection and Tracking via Cross-Scale Feature Aggregation Based on the Center Keypoint. Remote Sensing, 2021, 13, 1416.	4.0	6
81	ISAR Translational Motion Compensation with Simultaneous Range Alignment and Phase Adjustment in Low SNR Environments. , 2021, , .		5
82	A modified design method of pulse repetition frequency for synthetic aperture radar system based on the single point equivalent squint model. IET Radar, Sonar and Navigation, 2021, 15, 748-759.	1.8	0
83	Signal Subspace Reconstruction for DOA Detection Using Quantum-Behaved Particle Swarm Optimization. Remote Sensing, 2021, 13, 2560.	4.0	4
84	2-D Beam Steering Method for Squinted High-Orbit SAR Imaging. IEEE Transactions on Geoscience and Remote Sensing, 2021, 59, 4827-4840.	6.3	5
85	Robust CFAR Ship Detector Based on Bilateral-Trimmed-Statistics of Complex Ocean Scenes in SAR Imagery: A Closed-Form Solution. IEEE Transactions on Aerospace and Electronic Systems, 2021, 57, 1872-1890.	4.7	49
86	Fast Direction of Arrival Estimation for Uniform Circular Arrays With a Virtual Signal Subspace. IEEE Transactions on Aerospace and Electronic Systems, 2021, 57, 1731-1741.	4.7	15
87	Artificial Intelligence In Interferometric Synthetic Aperture Radar Phase Unwrapping: A Review. IEEE Geoscience and Remote Sensing Magazine, 2021, 9, 10-28.	9.6	50
88	CNN-LRP: Understanding Convolutional Neural Networks Performance for Target Recognition in SAR Images. Sensors, 2021, 21, 4536.	3.8	15
89	Ground Cartesian Back-Projection Algorithm for High Squint Diving TOPS SAR Imaging. IEEE Transactions on Geoscience and Remote Sensing, 2021, 59, 5812-5827.	6.3	30
90	Refocusing of Moving Ships in Squint SAR Images Based on Spectrum Orthogonalization. Remote Sensing, 2021, 13, 2807.	4.0	7

#	Article	IF	CITATIONS
91	DSDet: A Lightweight Densely Connected Sparsely Activated Detector for Ship Target Detection in High-Resolution SAR Images. Remote Sensing, 2021, 13, 2743.	4.0	20
92	High squint multichannel SAR imaging algorithm for high speed maneuvering platforms with small-aperture. Signal Processing, 2021, 185, 108078.	3.7	3
93	ISAR Signal Tracking and High-Resolution Imaging by Kalman Filtering. Remote Sensing, 2021, 13, 3389.	4.0	4
94	Focusing Challenges of Ships With Oscillatory Motions and Long Coherent Processing Interval. IEEE Transactions on Geoscience and Remote Sensing, 2021, 59, 6562-6572.	6.3	6
95	High Speed Maneuvering Platform Squint TOPS SAR Imaging Based on Local Polar Coordinate and Angular Division. Remote Sensing, 2021, 13, 3329.	4.0	1
96	Semi-supervised rotation forest based on ensemble margin theory for the classification of hyperspectral image with limited training data. Information Sciences, 2021, 575, 611-638.	6.9	26
97	Microwave Correlation Forward-Looking Super-Resolution Imaging Based on Compressed Sensing. IEEE Transactions on Geoscience and Remote Sensing, 2021, 59, 8326-8337.	6.3	17
98	Multisystem Interferometric Data Fusion Framework: A Three-Step Sensing Approach. IEEE Transactions on Geoscience and Remote Sensing, 2021, 59, 8501-8509.	6.3	9
99	SMOTE-Based Weighted Deep Rotation Forest for the Imbalanced Hyperspectral Data Classification. Remote Sensing, 2021, 13, 464.	4.0	14
100	The Recognition Framework of Deep Kernel Learning for Enclosed Remote Sensing Objects. IEEE Access, 2021, 9, 95585-95596.	4.2	2
101	Synthetic Aperture Radar Interference Based on Scene Fusion and Active Cancellation. IEEE Journal of Selected Topics in Applied Earth Observations and Remote Sensing, 2021, 14, 10375-10382.	4.9	2
102	Multi-Scale Feature Extraction and Total Variation Based Fusion Method For HSI and Lidar Data Classification. , 2021, , .		4
103	Azimuth Spectrum Reconstruction Algorithm for Multichannel Squint Sar on High Speed Airborne Platform. , 2021, , .		1
104	Ship Imaging based on Azimuth Ambiguity Resolving for High-Speed Maneuvering Platforms Sar with Small-Aperture. , 2021, , .		0
105	Design of Double-Mode Integrated Microwave Remote Sensor for Ocean Wave Observation. , 2021, , .		0
106	A Novel Forest Disater Monitoring Method Based on FCM and Neighborhood Factor Genetic Algorithm Using Multispectral Data. , 2021, , .		1
107	Parallel Ensemble Deep Learning for Real-Time Remote Sensing Video Multi-Target Detection. Remote Sensing, 2021, 13, 4377.	4.0	4
108	A Novel Clutter Covariance Matrix Estimation Method Based on Feature Subspace for Space-Based Early Warning Radar. IEEE Journal of Selected Topics in Applied Earth Observations and Remote Sensing, 2021, 14, 11217-11228.	4.9	5

#	Article	lF	CITATIONS
109	Fast Rotation Matching Method for SAR and Optical Images. IEEE Journal of Selected Topics in Applied Earth Observations and Remote Sensing, 2021, , 1-1.	4.9	0
110	Ocean Target Investigation Using Spaceborne SAR under Dual-Polarization Strip-map Mode. , 2021, , .		3
111	Parallel implementation of real-time ISAR imaging based on graphics processing units. , 2021, , .		0
112	A Two-Step Processing Method for Diving-Mode Squint SAR Imaging With Subaperture Data. IEEE Transactions on Geoscience and Remote Sensing, 2020, 58, 811-825.	6.3	7
113	Clutter Suppression via Subspace Projection for Spaceborne HRWS Multichannel SAR System. IEEE Geoscience and Remote Sensing Letters, 2020, 17, 1538-1542.	3.1	9
114	A Frequency-Domain Imaging Algorithm for Translational Variant Bistatic Forward-Looking SAR. IEEE Transactions on Geoscience and Remote Sensing, 2020, 58, 1502-1515.	6.3	20
115	InSAR Signal and Data Processing. Sensors, 2020, 20, 3801.	3.8	1
116	Focusing of Maneuvering High-Squint-Mode SAR Data Based on Equivalent Range Model and Wavenumber-Domain Imaging Algorithm. IEEE Journal of Selected Topics in Applied Earth Observations and Remote Sensing, 2020, 13, 2419-2433.	4.9	5
117	A Novel Image Fusion Method of Multi-Spectral and SAR Images for Land Cover Classification. Remote Sensing, 2020, 12, 3801.	4.0	31
118	A Novel Feature Extension Method for the Forest Disaster Monitoring Using Multispectral Data. Remote Sensing, 2020, 12, 2261.	4.0	11
119	ISAR Image Matching and Three-Dimensional Scattering Imaging Based on Extracted Dominant Scatterers. Remote Sensing, 2020, 12, 2699.	4.0	3
120	Time-Varying Baseline Error Estimation and Compensation in UAV SAR Interferometry Based on Time-Domain Subaperture of Raw Radar Data. IEEE Sensors Journal, 2020, 20, 12203-12216.	4.7	6
121	An adaptive-trimming-depth based CFAR detector of heterogeneous environment in SAR imagery. Remote Sensing Letters, 2020, 11, 730-738.	1.4	7
122	InSAR Phase Denoising: A Review of Current Technologies and Future Directions. IEEE Geoscience and Remote Sensing Magazine, 2020, 8, 64-82.	9.6	63
123	Antenna Beampattern With Range Null Control Using Weighted Frequency Diverse Array. IEEE Access, 2020, 8, 50107-50117.	4.2	15
124	A High-Squint TOPS SAR Imaging Algorithm for Maneuvering Platforms Based on Joint Time-Doppler Deramp Without Subaperture. IEEE Geoscience and Remote Sensing Letters, 2020, 17, 1899-1903.	3.1	13
125	A Special Issue on Synthetic Aperture Radar Interferometry [From the Guest Editors]. IEEE Geoscience and Remote Sensing Magazine, 2020, 8, 6-7.	9.6	15
126	Interferometric SAR Phase Filtering With SURE-Based Non-Local Method. IEEE Access, 2020, 8, 66722-66730.	4.2	1

#	Article	IF	CITATIONS
127	Cooperative Multitask Learning for Sparsity-Driven SAR Imagery and Nonsystematic Error Autocalibration. IEEE Transactions on Geoscience and Remote Sensing, 2020, 58, 5132-5147.	6.3	27
128	Correction of ``A Frequency-Domain Imaging Algorithm for Translational Variant Bistatic Forward-Looking SAR''. IEEE Transactions on Geoscience and Remote Sensing, 2020, , 1-1.	6.3	2
129	An Adaptive Hierarchical Detection Method for Ship Targets in High-Resolution SAR Images. Remote Sensing, 2020, 12, 303.	4.0	16
130	A Modified Range Model and Doppler Resampling Based Imaging Algorithm for High Squint SAR on Maneuvering Platforms. IEEE Geoscience and Remote Sensing Letters, 2020, 17, 1923-1927.	3.1	3
131	Focusing of MEO SAR Data Based on Principle of Optimal Imaging Coordinate System. IEEE Transactions on Geoscience and Remote Sensing, 2020, 58, 5477-5489.	6.3	7
132	Validating GEV Model for Reflection Symmetry-Based Ocean Ship Detection with Gaofen-3 Dual-Polarimetric Data. Remote Sensing, 2020, 12, 1148.	4.0	6
133	A Novel Reconstruction Method of K-Distributed Sea Clutter with Spatial–Temporal Correlation. Sensors, 2020, 20, 2377.	3.8	3
134	GF-3 data real-time processing method based on multi-satellite distributed data processing system. Journal of Central South University, 2020, 27, 842-852.	3.0	5
135	A novel 3-D radar imaging method based on sparse optimization. , 2020, , .		0
136	Spectral-Spatial Feature Extraction based CNN for Hyperspectral Image Classification. , 2020, , .		3
137	An Efficient MEO SAR Imaging Algorithm Based on Optimal Imaging Coordinate System. , 2020, , .		1
138	Achieving Millimetre Wave Seeker Performance Evaluation Based on the Real-Time Kinematic. Journal of Sensors, 2020, 2020, 1-13.	1.1	3
139	High-Resolution Imaging Based on Temporal-Spatial Stochastic Radiation Field and Compressive Sensing Theory. , 2020, , .		Ο
140	An Image-Domain Baseline Error Estimation Method for Azimuth Multi-Channel Sar. , 2020, , .		0
141	Ship Positioning and Radial Velocity Estimation for Spaceborne SAR Based on Energy Center Extraction. , 2020, , .		2
142	Feature Separation Based Rotation Forest for Hyperspectral Image Classification. , 2020, , .		0
143	A Two-Step Ship Target Detection Method in High-Resolution Sar Image Based on Coarse-to-Fine Mechanism. , 2020, , .		1
144	An Optimization Algorithm of Moving Targets Refocusing Via Parameter Estimation Dependence of Maximum Sharpness Principle After BP Integral. , 2020, , .		0

#	Article	IF	CITATIONS
145	Long Synthetic Aperture Passive Localization Using Azimuth Chirp-Rate Contour Map. , 2020, , .		1
146	Space Targets Rescaling Based on Bistatic ISAR System. , 2020, , .		0
147	New Algorithm for Near-Field ISAR Imaging. , 2020, , .		0
148	Two-Step Ensemble Based Class Noise Cleaning Method for Hyperspectral Image Classification. , 2020, , .		0
149	An Infinity-Norm-Based Phase Unwrapping Method with TSPA Framework for Multi-Baseline SAR Interferograms. , 2020, , .		Ο
150	Unambiguous Signal Reconstruction Algorithm for High Squint Multichannel SAR Mounted on High Speed Maneuvering Platforms. , 2020, , .		1
151	Clutter Suppression and Moving Target Radial Velocity Estimation Method for HRWS Multichannel System based on Subspace Projection. , 2020, , .		Ο
152	A Sidelobe Reduction Algorithm for SAR Imagery Formed by Fast Back Projection Algorithm Based on Spectrum Compression. , 2020, , .		1
153	A Fast Time-Domain SAR Imaging and Corresponding Autofocus Method Based on Hybrid Coordinate System. IEEE Transactions on Geoscience and Remote Sensing, 2019, 57, 8627-8640.	6.3	10
154	A Target Identification Method for the Millimeter Wave Seeker via Correlation Matching and Beam Pointing. Sensors, 2019, 19, 2530.	3.8	1
155	Highly Squinted MEO SAR Focusing Based on Extended Omega-K Algorithm and Modified Joint Time and Doppler Resampling. IEEE Transactions on Geoscience and Remote Sensing, 2019, 57, 9188-9200.	6.3	16
156	Focusing Improvement of Curved Trajectory Spaceborne SAR Based on Optimal LRWC Preprocessing and 2-D Singular Value Decomposition. IEEE Transactions on Geoscience and Remote Sensing, 2019, 57, 4246-4258.	6.3	18
157	Joint Method of ISAR Imaging and Scaling for Maneuvering Targets via Compressive Sensing. IEEE Sensors Journal, 2019, 19, 7300-7307.	4.7	5
158	High-Speed Maneuvering Platforms Squint Beam-Steering SAR Imaging Without Subaperture. IEEE Transactions on Geoscience and Remote Sensing, 2019, 57, 6974-6985.	6.3	17
159	A Multi-Perspective 3D Reconstruction Method with Single Perspective Instantaneous Target Attitude Estimation. Remote Sensing, 2019, 11, 1277.	4.0	6
160	Two-Step Accuracy Improvement of Motion Compensation for Airborne SAR With Ultrahigh Resolution and Wide Swath. IEEE Transactions on Geoscience and Remote Sensing, 2019, 57, 7148-7160.	6.3	38
161	A New Fast Factorized Back Projection Algorithm for Bistatic Forward-Looking SAR Imaging Based on Orthogonal Elliptical Polar Coordinate. IEEE Journal of Selected Topics in Applied Earth Observations and Remote Sensing, 2019, 12, 1508-1520.	4.9	13
162	A Novel Azimuth Doppler Signal Reconstruction Approach for the GEO-LEO Bi-Static Multi-Channel HRWS SAR System. IEEE Access, 2019, 7, 39539-39546.	4.2	13

#	Article	IF	CITATIONS
163	Refined Two-Stage Programming-Based Multi-Baseline Phase Unwrapping Approach Using Local Plane Model. Remote Sensing, 2019, 11, 491.	4.0	15
164	High-Rise Building 3D Reconstruction with the Wrapped Interferometric Phase. Sensors, 2019, 19, 1439.	3.8	3
165	A modified Omega-K algorithm for squint circular trace scanning SAR using improved range model. Signal Processing, 2019, 160, 59-65.	3.7	3
166	ISAR Imaging and Cross-Range Scaling for Maneuvering Targets by Using the NCS-NLS Algorithm. IEEE Sensors Journal, 2019, 19, 4889-4897.	4.7	16
167	A Novel Ionospheric TEC Estimation Method Based on L-Band ISAR Signal Processing. , 2019, , .		0
168	ISAR Imaging Based on Homotopy Re-Weighted â""1-Norm Minimization. , 2019, , .		1
169	A Convex Hull and Cluster-Analysis Based Fast Large-Scale Phase Unwrapping Method for Multibaseline Sar Interferograms. , 2019, , .		7
170	Applications of Baseband Azimuth Scaling on High Squint Beam Steering SAR Imaging with Contant Acceleration. , 2019, , .		0
171	Challenges of Ship Focusing with Long Coherence Processing Interval. , 2019, , .		1
172	Intersatellite cloud computing system for GF-3 SAR data real-time processing. , 2019, , .		3
173	A New Nonlinear Chirp Scaling Algorithm for Translational Variant Bistatic Forward-Looking SAR with Dive Trajectory. , 2019, , .		0
174	A New Approach for Optimization Selection of Spaceborne SAR Beam Position Parameters. , 2019, , .		0
175	Spaceâ€variant RCMC method for squint beamâ€steering SAR imaging on highâ€speed manoeuvring platforms. Electronics Letters, 2019, 55, 481-483.	1.0	1
176	A novel sidelobe-suppression algorithm for airborne synthetic aperture imaging ladar. Optics and Laser Technology, 2019, 111, 714-719.	4.6	6
177	Cross-range scaling for non-uniformly rotating targets by sharpness maximization. , 2019, 86, 29-35.		2
178	SAR platform positioning method based on improved Gauss–Newton–genetic hybrid algorithm. IET Radar, Sonar and Navigation, 2019, 13, 1154-1161.	1.8	2
179	A Imaging Passive Localization Method for Wideband Signal Based on SAR. , 2019, , .		4

Parameter estimation of QFM signal based on MPKF. , 2018, 76, 1-13.

#	Article	IF	CITATIONS
181	Cartesian Factorized Backprojection Algorithm for High-Resolution Spotlight SAR Imaging. IEEE Sensors Journal, 2018, 18, 1160-1168.	4.7	36
182	Moving Target Refocusing Algorithm in 2-D Wavenumber Domain After BP Integral. IEEE Geoscience and Remote Sensing Letters, 2018, 15, 127-131.	3.1	14
183	A Modified CSA Based on Joint Time-Doppler Resampling for MEO SAR Stripmap Mode. IEEE Transactions on Geoscience and Remote Sensing, 2018, 56, 3573-3586.	6.3	21
184	Focusing of Medium-Earth-Orbit SAR Using an ASE-Velocity Model Based on MOCO Principle. IEEE Transactions on Geoscience and Remote Sensing, 2018, 56, 3963-3975.	6.3	16
185	An Analytical Resolution Evaluation Approach for Bistatic GEOSAR Based on Local Feature of Ambiguity Function. IEEE Transactions on Geoscience and Remote Sensing, 2018, 56, 2159-2169.	6.3	17
186	Range–Doppler reconstruction for frequency agile and PRFâ€ <del>j</del> ittering radar. IET Radar, Sonar and Navigation, 2018, 12, 348-352.	1.8	41
187	SAR Target Configuration Recognition via Two-Stage Sparse Structure Representation. IEEE Transactions on Geoscience and Remote Sensing, 2018, 56, 2220-2232.	6.3	28
188	A Novel Weighted Doppler Centroid Estimation Approach Based on Electromagnetic Scattering Model for Multichannel in Azimuth HRWS SAR System. IEEE Transactions on Geoscience and Remote Sensing, 2018, 56, 5015-5034.	6.3	10
189	Characteristics Analysis and Image Processing for Full-Polarization Synthetic Aperture Radar Based on Electromagnetic Scattering From Flat Horizontal Perfect Electric Conducting Reflector. IEEE Transactions on Geoscience and Remote Sensing, 2018, 56, 313-327.	6.3	5
190	Analysis of angle vibration effects on imaging quality of synthetic aperture ladar. Optik, 2018, 157, 298-305.	2.9	1
191	Multi-channel scan mode and imaging algorithm for synthetic aperture ladar. Optik, 2018, 155, 225-232.	2.9	2
192	Extraction of Anisotropic Characteristics of Scattering Centers and Feature Enhancement in Wide-Angle SAR Imagery Based on the Iterative Re-Weighted Tikhonov Regularization. Remote Sensing, 2018, 10, 2066.	4.0	8
193	Multi-View Electromagnetic Imagining. , 2018, , .		1
194	Micro-Doppler Feature Extraction of Inverse Synthetic Aperture Imaging Laser Radar Using Singular-Spectrum Analysis. Sensors, 2018, 18, 3303.	3.8	9
195	A Channel Phase Error Correction Method Based on Joint Quality Function of GF-3 SAR Dual-Channel Images. Sensors, 2018, 18, 3131.	3.8	10
196	Joint High-Resolution Range and DOA Estimation via MUSIC Method Based on Virtual Two-Dimensional Spatial Smoothing for OFDM Radar. International Journal of Antennas and Propagation, 2018, 2018, 1-9.	1.2	5
197	Terahertz Image Detection with the Improved Faster Region-Based Convolutional Neural Network. Sensors, 2018, 18, 2327.	3.8	42
198	SAR Target Configuration Recognition via Product Sparse Representation. Sensors, 2018, 18, 3535.	3.8	1

#	Article	IF	CITATIONS
199	A Real-Time Imaging Algorithm Based on Sub-Aperture CS-Dechirp for GF3-SAR Data. Sensors, 2018, 18, 2562.	3.8	24
200	A Novel MIMO–SAR Solution Based on Azimuth Phase Coding Waveforms and Digital Beamforming. Sensors, 2018, 18, 3374.	3.8	7
201	Multi-Channel Synthetic Aperture Radar Imaging of Ground Moving Targets Using Compressive Sensing. IEEE Access, 2018, 6, 66134-66142.	4.2	6
202	A Novel Focus Approach for Squint Mode Multi-Channel in Azimuth High-Resolution and Wide-Swath SAR Imaging Processing. IEEE Access, 2018, 6, 74303-74319.	4.2	6
203	Airborne Bistatic Forward-Looking SAR Using the Polynomial NCS Algorithm. , 2018, 2, 1-4.		8
204	Efficient Doppler ambiguity resolver for video SAR. Electronics Letters, 2018, 54, 443-445.	1.0	3
205	Real-time implementation of inverse synthetic aperture radar imaging using field programmable gate array and digital signal processors. Review of Scientific Instruments, 2018, 89, 074704.	1.3	0
206	Coherent Auto-Calibration of APE and NsRCM under Fast Back-Projection Image Formation for Airborne SAR Imaging inHighly-Squint Angle. Remote Sensing, 2018, 10, 321.	4.0	6
207	Ultrahigh Range Resolution ISAR Processing by Using KT–TCS Algorithm. IEEE Sensors Journal, 2018, 18, 8311-8317.	4.7	13
208	A two-dimensional phase coding for range ambiguity suppression. , 2018, 81, 155-162.		6
209	A Frequency Domain Backprojection Algorithm Based on Local Cartesian Coordinate and Subregion Range Migration Correction for High-Squint SAR Mounted on Maneuvering Platforms. IEEE Transactions on Geoscience and Remote Sensing, 2018, 56, 7086-7101.	6.3	16
210	SAR Target Configuration Recognition via Discriminative Statistical Dictionary Learning. IEEE Journal of Selected Topics in Applied Earth Observations and Remote Sensing, 2018, 11, 4218-4229.	4.9	7
211	Wide-scene airborne ladar imaging exploiting the synthetic aperture technique with terrain observation by progressive scans. Optical Engineering, 2018, 57, 1.	1.0	4
212	Optical and electrical properties of short-pitch solar cells with finite-difference frequency-domain method. Wuli Xuebao/Acta Physica Sinica, 2018, 67, 178102.	0.5	0
213	A Two-Dimensional Beam-Steering Method to Simultaneously Consider Doppler Centroid and Ground Observation in GEOSAR. IEEE Journal of Selected Topics in Applied Earth Observations and Remote Sensing, 2017, 10, 161-167.	4.9	16
214	Improved Signal Reconstruction Algorithm for Multichannel SAR Based on the Doppler Spectrum Estimation. IEEE Journal of Selected Topics in Applied Earth Observations and Remote Sensing, 2017, 10, 1425-1442.	4.9	36
215	Thorough Understanding Property of Bistatic Forward-Looking High-Speed Maneuvering Platform SAR. IEEE Transactions on Aerospace and Electronic Systems, 2017, 53, 1826-1845.	4.7	20
216	A Novel Doppler Chirp Rate and Baseline Estimation Approach in the Time Domain Based on Weighted Local Maximum-Likelihood for an MC-HRWS SAR System. IEEE Geoscience and Remote Sensing Letters, 2017, 14, 299-303.	3.1	18

#	Article	IF	CITATIONS
217	Maneuvering target imaging and scaling by using sparse inverse synthetic aperture. Signal Processing, 2017, 137, 149-159.	3.7	20
218	Analysis of Airborne Synthetic Aperture Ladar Imaging with Platform Vibration. Optik, 2017, 140, 171-177.	2.9	9
219	Sequence design for high squint spotlight SAR imaging on manoeuvring descending trajectory. IET Radar, Sonar and Navigation, 2017, 11, 219-225.	1.8	2
220	A Modified Equivalent Range Model and Wavenumber-Domain Imaging Approach for High-Resolution-High-Squint SAR With Curved Trajectory. IEEE Transactions on Geoscience and Remote Sensing, 2017, 55, 3721-3734.	6.3	42
221	Full-Aperture Focusing of Very High Resolution Spaceborne-Squinted Sliding Spotlight SAR Data. IEEE Transactions on Geoscience and Remote Sensing, 2017, 55, 3309-3321.	6.3	18
222	A 2-D Space-Variant Motion Estimation and Compensation Method for Ultrahigh-Resolution Airborne Stepped-Frequency SAR With Long Integration Time. IEEE Transactions on Geoscience and Remote Sensing, 2017, 55, 6390-6401.	6.3	54
223	Performance Improvement and System Design of Geo-SAR Using the Yaw Steering. IEEE Sensors Journal, 2017, 17, 6268-6278.	4.7	7
224	Paired echo suppression algorithm in helicopterâ€borne SAR imaging. IET Radar, Sonar and Navigation, 2017, 11, 1605-1612.	1.8	7
225	A Novel Two-Step Approach of Error Estimation for Stepped-Frequency MIMO-SAR. IEEE Geoscience and Remote Sensing Letters, 2017, 14, 2290-2294.	3.1	13
226	FM sequence optimisation of chaoticâ€based random stepped frequency signal in throughâ€theâ€wall radar. IET Signal Processing, 2017, 11, 830-837.	1.5	9
227	Enhanced ISAR Imaging and Motion Estimation With Parametric and Dynamic Sparse Bayesian Learning. IEEE Transactions on Computational Imaging, 2017, 3, 940-952.	4.4	47
228	FPGA Implementation of Real-Time Compressive Sensing with Partial Fourier Dictionary. International Journal of Antennas and Propagation, 2016, 2016, 1-12.	1.2	19
229	Focusing of Spotlight Tandem-Configuration Bistatic Data with Frequency Scaling Algorithm. International Journal of Antennas and Propagation, 2016, 2016, 1-15.	1.2	0
230	Ionosphere correction algorithm for spaceborne SAR imaging. Journal of Systems Engineering and Electronics, 2016, 27, 993-1000.	2.2	2
231	Doppler ambiguity removal and ISAR imaging of group targets with sparse decomposition. IET Radar, Sonar and Navigation, 2016, 10, 1711-1719.	1.8	4
232	Full aperture imaging algorithm for highly squinted TOPS SAR. Journal of Systems Engineering and Electronics, 2016, 27, 1168-1175.	2.2	4
233	A Parameter Optimization Model for Geosynchronous SAR Sensor in Aspects of Signal Bandwidth and Integration Time. IEEE Geoscience and Remote Sensing Letters, 2016, 13, 1374-1378.	3.1	20

A method for extracting amplitude attribute of scattering centers in SAR. , 2016, , .

3

#	Article	IF	CITATIONS
235	GEO spaceborne-airborne BiSAR resolution analysis and bandwidth and synthetic aperture time design. , 2016, , .		1
236	Moving target detection for frequency agility radar by sparse reconstruction. Review of Scientific Instruments, 2016, 87, 094703.	1.3	15
237	An Inverse Extended Omega-K Algorithm for SAR Raw Data Simulation With Trajectory Deviations. IEEE Geoscience and Remote Sensing Letters, 2016, 13, 826-830.	3.1	8
238	3D Geometry and Motion Estimations of Maneuvering Targets for Interferometric ISAR With Sparse Aperture. IEEE Transactions on Image Processing, 2016, 25, 2005-2020.	9.8	66
239	A Frequency-Domain Imaging Algorithm for Highly Squinted SAR Mounted on Maneuvering Platforms With Nonlinear Trajectory. IEEE Transactions on Geoscience and Remote Sensing, 2016, 54, 4023-4038.	6.3	72
240	An Improved Range Model and Omega-K-Based Imaging Algorithm for High-Squint SAR With Curved Trajectory and Constant Acceleration. IEEE Geoscience and Remote Sensing Letters, 2016, 13, 656-660.	3.1	31
241	Twoâ€dimensional autofocus technique for highâ€resolution spotlight synthetic aperture radar. IET Signal Processing, 2016, 10, 699-707.	1.5	19
242	Cartesian factorized backprojection algorithm for synthetic aperture radar. , 2016, , .		7
243	Phase adjustment for polarimetric ISAR with compressive sensing. IEEE Transactions on Aerospace and Electronic Systems, 2016, 52, 1592-1606.	4.7	11
244	A TSVD-NCS Algorithm in Range-Doppler Domain for Geosynchronous Synthetic Aperture Radar. IEEE Geoscience and Remote Sensing Letters, 2016, 13, 1631-1635.	3.1	27
245	Equivalent hyperbolic range model for synthetic aperture radar with curved track. Electronics Letters, 2016, 52, 1252-1253.	1.0	5
246	A novel digital beam-forming (DBF) method for multi-modes MIMO-SAR. , 2016, , .		6
247	A New SAR–GMTI High-Accuracy Focusing and Relocation Method Using Instantaneous Interferometry. IEEE Transactions on Geoscience and Remote Sensing, 2016, 54, 5564-5577.	6.3	9
248	Simultaneous Stationary Scene Imaging and Ground Moving Target Indication for High-Resolution Wide-Swath SAR System. IEEE Transactions on Geoscience and Remote Sensing, 2016, 54, 4224-4239.	6.3	32
249	A Novel Motion Compensation Approach for Airborne Spotlight SAR of High-Resolution and High-Squint Mode. IEEE Geoscience and Remote Sensing Letters, 2016, , 1-5.	3.1	22
250	Multiple-input multiple-output synthetic aperture ladar system for wide-range swath with high azimuth resolution. Applied Optics, 2016, 55, 1401.	2.1	2
251	A Modified <inline-formula> <tex-math notation="LaTeX">\$omega\$</tex-math> </inline-formula> – <inline-formula> <tex-math notation="LaTeX">\$k\$</tex-math> </inline-formula> Algorithm for HS-SAR Small-Aperture Data Imaging. IEEE Transactions on	6.3	22
252	Geoscience and Remote Sensing, 2016, 54, 3710-3721. Processing of Very High Resolution Spaceborne Sliding Spotlight SAR Data Using Velocity Scaling. IEEE Transactions on Geoscience and Remote Sensing, 2016, 54, 1505-1518.	6.3	42

#	Article	IF	CITATIONS
253	Focusing of Highly Squinted SAR Data With Frequency Nonlinear Chirp Scaling. IEEE Geoscience and Remote Sensing Letters, 2016, 13, 23-27.	3.1	37
254	Joint approach of translational and rotational phase error corrections for highâ€resolution inverse synthetic aperture radar imaging using minimumâ€entropy. IET Radar, Sonar and Navigation, 2016, 10, 586-594.	1.8	18
255	Small-aperture imaging for high squint SAR based on modified Omega-K algorithm. , 2015, , .		0
256	Real-time implementation of frequency-modulated continuous-wave synthetic aperture radar imaging using field programmable gate array. Review of Scientific Instruments, 2015, 86, 064706.	1.3	1
257	The design and implementation of a multi-waveform radar echo simulator. Review of Scientific Instruments, 2015, 86, 104702.	1.3	1
258	A novel Doppler chirp rate and baseline estimation approach in time domain for multi-channel in azimuth HRWS SAR system. , 2015, , .		2
259	Systematic analyses of challenges and solutions in geosynchronous synthetic aperture radar. , 2015, , .		2
260	Joint Multichannel Motion Compensation Method for MIMO SAR 3D Imaging. International Journal of Antennas and Propagation, 2015, 2015, 1-7.	1.2	2
261	Interesting components detection for space satellites from inverse synthetic aperture radar image via feature probabilistic estimation. IET Image Processing, 2015, 9, 506-515.	2.5	1
262	A sub-aperture imaging algorithm for highly squinted SAR based on frequency phase correction. , 2015, , .		3
263	A novel deramp space-time adaptive processing method for multichannel SAR-GMTI. , 2015, , .		1
264	Enhanced target extraction in strong clutter scene. , 2015, , .		0
265	A modified fast factorized back projection algorithm for the spotlight SAR imaging. , 2015, , .		2
266	Fast raw data simulator of extended scenes for bistatic forward-looking synthetic aperture radar with constant acceleration. , 2015, , .		0
267	Genetic algorithm based multi-band SAR parameter optimization for MTD. , 2015, , .		0
268	lonosphere correction algorithm for P-band spaceborne SAR imaging. , 2015, , .		0
269	Measurement and Correction of the Ionospheric TEC in P-Band ISAR Imaging. IEEE Geoscience and Remote Sensing Letters, 2015, 12, 1755-1759.	3.1	7
270	An interpolation-free FFBP algorithm for spotlight SAR processing. , 2015, , .		0

#	Article	IF	CITATIONS
271	A coordinate-transform based FFBP algorithm for high-resolution spotlight SAR imaging. Science China Information Sciences, 2015, 58, 1-11.	4.3	3
272	A raw data simulator for Bistatic Forward-looking High-speed Maneuvering-platform SAR. Signal Processing, 2015, 117, 151-164.	3.7	32
273	Analysis on parameters and imaging algorithm of squint circular trace scanning SAR. , 2015, , .		2
274	Expediting backâ€projection algorithm for circular SAR imaging. Electronics Letters, 2015, 51, 785-787.	1.0	5
275	A fast implementation method for the FFBP algorithm. , 2015, , .		0
276	Highâ€resolution inverse synthetic aperture radar imaging of manoeuvring targets with sparse aperture. Electronics Letters, 2015, 51, 287-289.	1.0	11
277	A Novel Mixed-Norm Multibaseline Phase-Unwrapping Algorithm Based on Linear Programming. IEEE Geoscience and Remote Sensing Letters, 2015, 12, 1086-1090.	3.1	19
278	Airborne SAR Moving Target Signatures and Imagery Based on LVD. IEEE Transactions on Geoscience and Remote Sensing, 2015, 53, 5958-5971.	6.3	41
279	A Robust Imaging Algorithm for Squint Mode Multi-Channel High-Resolution and Wide-Swath SAR With Hybrid Baseline and Fluctuant Terrain. IEEE Journal on Selected Topics in Signal Processing, 2015, 9, 1583-1598.	10.8	23
280	Factorised polarâ€format backâ€projection algorithm. IET Radar, Sonar and Navigation, 2015, 9, 875-880.	1.8	2
281	Autofocus algorithm using blind homomorphic deconvolution for synthetic aperture radar imaging. IET Radar, Sonar and Navigation, 2015, 9, 900-906.	1.8	4
282	Threeâ€dimensional interferometric inverse synthetic aperture radar imaging with limited pulses by exploiting joint sparsity. IET Radar, Sonar and Navigation, 2015, 9, 692-701.	1.8	20
283	A High-Order Phase Correction Approach for Focusing HS-SAR Small-Aperture Data of High-Speed Moving Platforms. IEEE Journal of Selected Topics in Applied Earth Observations and Remote Sensing, 2015, 8, 4551-4561.	4.9	24
284	High-Resolution Inverse Synthetic Aperture Radar Imaging and Scaling With Sparse Aperture. IEEE Journal of Selected Topics in Applied Earth Observations and Remote Sensing, 2015, 8, 4010-4027.	4.9	72
285	A weighted contrast enhancement autofocus algorithm. , 2015, , .		3
286	Wide angle radar imaging under low SNR via sparsity enhanced non-negative matrix factorization. , 2015, , .		0
287	Spectrum Compression Space–Time Adaptive Processing for TOPS SAR System. IEEE Geoscience and Remote Sensing Letters, 2015, 12, 434-438.	3.1	10
288	ISAR Cross-Range Scaling by Using Sharpness Maximization. IEEE Geoscience and Remote Sensing Letters, 2015, 12, 165-169.	3.1	56

#	Article	IF	CITATIONS
289	Robust Clutter Suppression and Moving Target Imaging Approach for Multichannel in Azimuth High-Resolution and Wide-Swath Synthetic Aperture Radar. IEEE Transactions on Geoscience and Remote Sensing, 2015, 53, 687-709.	6.3	51
290	A Cluster-Analysis-Based Noise-Robust Phase-Unwrapping Algorithm for Multibaseline Interferograms. IEEE Transactions on Geoscience and Remote Sensing, 2015, 53, 494-504.	6.3	37
291	Sparse Regularization of Interferometric Phase and Amplitude for InSAR Image Formation Based on Bayesian Representation. IEEE Transactions on Geoscience and Remote Sensing, 2015, 53, 2123-2136.	6.3	31
292	MIMO-Based Forward-Looking SAR Imaging Algorithm and Simulation. International Journal of Antennas and Propagation, 2014, 2014, 1-9.	1.2	5
293	OTHR Spectrum Reconstruction of Maneuvering Target with Compressive Sensing. International Journal of Antennas and Propagation, 2014, 2014, 1-10.	1.2	4
294	Property Analysis of MIMO-Based Missile-Borne Forward-Looking SAR. International Journal of Antennas and Propagation, 2014, 2014, 1-9.	1.2	4
295	An Efficient Signal Reconstruction Algorithm for Stepped Frequency MIMO-SAR in the Spotlight and Sliding Spotlight Modes. International Journal of Antennas and Propagation, 2014, 2014, 1-8.	1.2	4
296	Phase adjustment and isar imaging of maneuvering targets with sparse apertures. IEEE Transactions on Aerospace and Electronic Systems, 2014, 50, 1955-1973.	4.7	48
297	Analysis of threeâ€component decomposition to compact polarimetric synthetic aperture radar. IET Radar, Sonar and Navigation, 2014, 8, 685-691.	1.8	18
298	3-D ghost imaging with microwave radar. , 2014, , .		6
299	Multichannel HRWS SAR Imaging Based on Range-Variant Channel Calibration and Multi-Doppler-Direction Restriction Ambiguity Suppression. IEEE Transactions on Geoscience and Remote Sensing, 2014, 52, 4306-4327.	6.3	79
300	A novel beam direction determination method for minimizing Doppler centroid in GEO SAR. , 2014, , .		2
301	An Azimuth Frequency Non-Linear Chirp Scaling (FNCS) Algorithm for TOPS SAR Imaging With High Squint Angle. IEEE Journal of Selected Topics in Applied Earth Observations and Remote Sensing, 2014, 7, 213-221.	4.9	33
302	A subaperture imaging scheme for wide azimuth beam airborne SAR based on modified RMA with motion compensation. , 2014, , .		2
303	Sparse aperture inverse synthetic aperture radar imaging of manoeuvring targets with compensation of migration through range cells. IET Radar, Sonar and Navigation, 2014, 8, 1164-1176.	1.8	19
304	Minimum-Entropy-Based Autofocus Algorithm for SAR Data Using Chebyshev Approximation and Method of Series Reversion, and Its Implementation in a Data Processor. IEEE Transactions on Geoscience and Remote Sensing, 2014, 52, 1719-1728.	6.3	50
305	Azimuth Resampling Processing for Highly Squinted Synthetic Aperture Radar Imaging With Several Modes. IEEE Transactions on Geoscience and Remote Sensing, 2014, 52, 4339-4352.	6.3	39
306	Stepped frequency synthetic preprocessing algorithm for inverse synthetic aperture radar imaging in fast moving target echo model. IET Radar, Sonar and Navigation, 2014, 8, 864-874.	1.8	5

#	Article	IF	CITATIONS
307	Uniform rotational motion compensation for inverse synthetic aperture radar targets from image domain. , 2014, , .		0
308	A novel signal reconstructing method for radar targets. , 2014, , .		0
309	A 2-D Space-Variant Chirp Scaling Algorithm Based on the RCM Equalization and Subband Synthesis to Process Geosynchronous SAR Data. IEEE Transactions on Geoscience and Remote Sensing, 2014, 52, 4868-4880.	6.3	78
310	Super-resolution imaging algorithm based on attributed scattering center model. , 2014, , .		8
311	Sparse Apertures ISAR Imaging and Scaling for Maneuvering Targets. IEEE Journal of Selected Topics in Applied Earth Observations and Remote Sensing, 2014, 7, 2942-2956.	4.9	85
312	Polarimetric Target Decomposition Based on Attributed Scattering Center Model for Synthetic Aperture Radar Targets. IEEE Geoscience and Remote Sensing Letters, 2014, 11, 2095-2099.	3.1	41
313	Imaging of missile-borne bistatic forward-looking SAR. , 2014, , .		4
314	Transient interference excision and spectrum reconstruction with partial samples for overâ€theâ€horizon radar. IET Radar, Sonar and Navigation, 2014, 8, 547-556.	1.8	7
315	Amplitudeâ€phase discontinuity calibration for phased array radar in varying jamming environment. IET Signal Processing, 2014, 8, 729-737.	1.5	1
316	Deramp Space–Time Adaptive Processing for Multichannel SAR Systems. IEEE Geoscience and Remote Sensing Letters, 2014, 11, 1448-1452.	3.1	28
317	Squinted TOPS SAR Imaging Based on Modified Range Migration Algorithm and Spectral Analysis. IEEE Geoscience and Remote Sensing Letters, 2014, 11, 1707-1711.	3.1	27
318	Precise Cross-Range Scaling for ISAR Images Using Feature Registration. IEEE Geoscience and Remote Sensing Letters, 2014, 11, 1792-1796.	3.1	27
319	A Novel Moving Target Imaging Algorithm for HRWS SAR Based on Local Maximum-Likelihood Minimum Entropy. IEEE Transactions on Geoscience and Remote Sensing, 2014, 52, 5333-5348.	6.3	29
320	The range alignment approach for signal acquisition system. IEICE Electronics Express, 2014, 11, 20140304-20140304.	0.8	1
321	A weighted eigenvector autofocus method for sparse-aperture ISAR imaging. Eurasip Journal on Advances in Signal Processing, 2013, 2013, .	1.7	6
322	A novel modified Omega-K algorithm for circular trajectory scanning SAR imaging using series reversion. Eurasip Journal on Advances in Signal Processing, 2013, 2013, .	1.7	15
323	Focusing of tandem bistatic SAR data using the chirp-scaling algorithm. Eurasip Journal on Advances in Signal Processing, 2013, 2013, .	1.7	3
324	Translational motion compensation for ISAR imaging under low SNR by minimum entropy. Eurasip Journal on Advances in Signal Processing, 2013, 2013, .	1.7	43

#	Article	IF	CITATIONS
325	Beam Steering SAR Data Processing by a Generalized PFA. IEEE Transactions on Geoscience and Remote Sensing, 2013, 51, 4366-4377.	6.3	43
326	New Applications of Omega-K Algorithm for SAR Data Processing Using Effective Wavelength at High Squint. IEEE Transactions on Geoscience and Remote Sensing, 2013, 51, 3156-3169.	6.3	41
327	Multichannel Full-Aperture Azimuth Processing for Beam Steering SAR. IEEE Transactions on Geoscience and Remote Sensing, 2013, 51, 4761-4778.	6.3	42
328	An Improved SAC Algorithm Based on the Range-Keystone Transform for Doppler Rate Estimation. IEEE Geoscience and Remote Sensing Letters, 2013, 10, 741-745.	3.1	24
329	Robust Autofocusing Approach for Highly Squinted SAR Imagery Using the Extended Wavenumber Algorithm. IEEE Transactions on Geoscience and Remote Sensing, 2013, 51, 5031-5046.	6.3	70
330	A New Algorithm of ISAR Imaging for Maneuvering Targets with Low SNR. IEEE Transactions on Aerospace and Electronic Systems, 2013, 49, 543-557.	4.7	84
331	Correction to "An Azimuth-Dependent Phase Gradient Autofocus (APGA) Algorithm for Airborne/Stationary BiSAR Imagery―[Nov 13 1290-1294]. IEEE Geoscience and Remote Sensing Letters, 2013, 10, 1622-1622.	3.1	0
332	An Azimuth-Dependent Phase Gradient Autofocus (APGA) Algorithm for Airborne/Stationary BiSAR Imagery. IEEE Geoscience and Remote Sensing Letters, 2013, 10, 1290-1294.	3.1	31
333	Integrating Autofocus Techniques With Fast Factorized Back-Projection for High-Resolution Spotlight SAR Imaging. IEEE Geoscience and Remote Sensing Letters, 2013, 10, 1394-1398.	3.1	66
334	A Unified Focusing Algorithm for Several Modes of SAR Based on FrFT. IEEE Transactions on Geoscience and Remote Sensing, 2013, 51, 3139-3155.	6.3	37
335	Sparse Subband Imaging of Space Targets in High-Speed Motion. IEEE Transactions on Geoscience and Remote Sensing, 2013, 51, 4144-4154.	6.3	24
336	Compensation for the NsRCM and Phase Error After Polar Format Resampling for Airborne Spotlight SAR Raw Data of High Resolution. IEEE Geoscience and Remote Sensing Letters, 2013, 10, 165-169.	3.1	68
337	The Space-Variant Phase-Error Matching Map-Drift Algorithm for Highly Squinted SAR. IEEE Geoscience and Remote Sensing Letters, 2013, 10, 845-849.	3.1	27
338	Robust Ground Moving-Target Imaging Using Deramp–Keystone Processing. IEEE Transactions on Geoscience and Remote Sensing, 2013, 51, 966-982.	6.3	183
339	A Fast Phase Unwrapping Method for Large-Scale Interferograms. IEEE Transactions on Geoscience and Remote Sensing, 2013, 51, 4240-4248.	6.3	37
340	Azimuth Overlapped Subaperture Algorithm in Frequency Domain for Highly Squinted Synthetic Aperture Radar. IEEE Geoscience and Remote Sensing Letters, 2013, 10, 692-696.	3.1	9
341	A Robust Channel-Calibration Algorithm for Multi-Channel in Azimuth HRWS SAR Imaging Based on Local Maximum-Likelihood Weighted Minimum Entropy. IEEE Transactions on Image Processing, 2013, 22, 5294-5305.	9.8	45
342	Focus Improvement of High-Squint SAR Based on Azimuth Dependence of Quadratic Range Cell Migration Correction. IEEE Geoscience and Remote Sensing Letters, 2013, 10, 150-154.	3.1	47

#	Article	IF	CITATIONS
343	Azimuth scaling for inverse synthetic aperture radar images with feature registration. , 2013, , .		1
344	Fusion of multiâ€aspect radar images via sparse nonâ€negative matrix factorisation. Electronics Letters, 2013, 49, 1635-1637.	1.0	5
345	Imaging algorithm for circular trace scanning synthetic aperture radar using modified hyperbolic range equation. Electronics Letters, 2013, 49, 1296-1298.	1.0	5
346	A nonlinear chirp scaling algorithm for tandem bistatic SAR. , 2013, , .		3
347	Cross-range scaling combining motion compensation for ISAR imaging. , 2013, , .		1
348	A SIFT Algorithm for Bistatic SAR Imaging in a Spaceborne. Journal of Radars, 2013, 2, 14-22.	0.0	0
349	Chirp scaling algorithm for GEO SAR based on fourth-order range equation. Electronics Letters, 2012, 48, 41.	1.0	25
350	A Robust Motion Compensation Approach for UAV SAR Imagery. IEEE Transactions on Geoscience and Remote Sensing, 2012, 50, 3202-3218.	6.3	149
351	A New Look at Loffeld's Bistatic Formula in Tandem Configuration. IEEE Geoscience and Remote Sensing Letters, 2012, 9, 710-714.	3.1	8
352	Transient interference excision and spectrum reconstruction for OTHR. Electronics Letters, 2012, 48, 42.	1.0	20
353	Wavenumber-Domain Autofocusing for Highly Squinted UAV SAR Imagery. IEEE Sensors Journal, 2012, 12, 1574-1588.	4.7	94
354	High-Resolution ISAR Imaging by Exploiting Sparse Apertures. IEEE Transactions on Antennas and Propagation, 2012, 60, 997-1008.	5.1	160
355	ISAR imaging via sparse frequency-stepped chirp signal. Science China Information Sciences, 2012, 55, 877-888.	4.3	6
356	Coherent processing for ISAR imaging with sparse apertures. Science China Information Sciences, 2012, 55, 1898-1909.	4.3	3
357	Performance improvement in multi-ship imaging for ScanSAR based on sparse representation. Science China Information Sciences, 2012, 55, 1860-1875.	4.3	5
358	High-Resolution Radar Imaging of Air Targets From Sparse Azimuth Data. IEEE Transactions on Aerospace and Electronic Systems, 2012, 48, 1643-1655.	4.7	37
359	A Novel Method for Imaging of Group Targets Moving in a Formation. IEEE Transactions on Geoscience and Remote Sensing, 2012, 50, 221-231.	6.3	33
360	Echo Model Analyses and Imaging Algorithm for High-Resolution SAR on High-Speed Platform. IEEE Transactions on Geoscience and Remote Sensing, 2012, 50, 933-950.	6.3	62

#	Article	IF	CITATIONS
361	Parameter estimation of moving targets in the SAR system with a low PRF sampling rate. Science China Information Sciences, 2012, 55, 337-347.	4.3	7
362	A new signal model for a wideband synthetic aperture imaging sensor. Canadian Journal of Remote Sensing, 2011, 37, 171-183.	2.4	5
363	Focus Improvement of Highly Squinted Data Based on Azimuth Nonlinear Scaling. IEEE Transactions on Geoscience and Remote Sensing, 2011, 49, 2308-2322.	6.3	107
364	High-Resolution ISAR Imaging With Sparse Stepped-Frequency Waveforms. IEEE Transactions on Geoscience and Remote Sensing, 2011, 49, 4630-4651.	6.3	154
365	Interference Suppression Algorithm for SAR Based on Time–Frequency Transform. IEEE Transactions on Geoscience and Remote Sensing, 2011, 49, 3765-3779.	6.3	72
366	Exact analytical two-dimensional spectrum for bistatic synthetic aperture radar in tandem configuration. IET Radar, Sonar and Navigation, 2011, 5, 349.	1.8	10
367	Novel range profile synthesis algorithm for linearly stepped-frequency modulated inversed synthetic aperture radar imaging of remote manoeuvring target. IET Radar, Sonar and Navigation, 2011, 5, 496.	1.8	9
368	Stepped-frequency inverse synthetic aperture radar imaging based on adjacent pulse correlation integration and coherent processing. IET Signal Processing, 2011, 5, 632.	1.5	10
369	Focusing of Tandem Bistatic-Configuration Data With Range Migration Algorithm. IEEE Geoscience and Remote Sensing Letters, 2011, 8, 88-92.	3.1	13
370	Extended NCS Based on Method of Series Reversion for Imaging of Highly Squinted SAR. IEEE Geoscience and Remote Sensing Letters, 2011, 8, 446-450.	3.1	35
371	ISAR Imaging via Sparse Probing Frequencies. IEEE Geoscience and Remote Sensing Letters, 2011, 8, 451-455.	3.1	69
372	Sliding Spotlight and TOPS SAR Data Processing Without Subaperture. IEEE Geoscience and Remote Sensing Letters, 2011, 8, 1036-1040.	3.1	64
373	A Novel Strategy of Nonnegative-Matrix-Factorization-Based Polarimetric Ship Detection. IEEE Geoscience and Remote Sensing Letters, 2011, 8, 1085-1089.	3.1	11
374	A Variable-Decoupling- and MSR-Based Imaging Algorithm for a SAR of Curvilinear Orbit. IEEE Geoscience and Remote Sensing Letters, 2011, 8, 1145-1149.	3.1	18
375	Bayesian Inverse Synthetic Aperture Radar Imaging. IEEE Geoscience and Remote Sensing Letters, 2011, 8, 1150-1154.	3.1	109
376	Using Derivatives of an Implicit Function to Obtain the Stationary Phase of the Two-Dimensional Spectrum for Bistatic SAR Imaging. IEEE Geoscience and Remote Sensing Letters, 2011, 8, 1165-1169.	3.1	8
377	New Parameter Estimation and Detection Algorithm for High Speed Small Target. IEEE Transactions on Aerospace and Electronic Systems, 2011, 47, 214-224.	4.7	111
378	High Resolution ISAR Imaging of Targets with Rotating Parts. IEEE Transactions on Aerospace and Electronic Systems, 2011, 47, 2530-2543.	4.7	87

#	Article	IF	CITATIONS
379	Narrow-band radar imaging of spinning targets. Science China Information Sciences, 2011, 54, 873-883.	4.3	25
380	Generating dense and super-resolution ISAR image by combining bandwidth extrapolation and compressive sensing. Science China Information Sciences, 2011, 54, 2158-2169.	4.3	16
381	Lv's Distribution: Principle, Implementation, Properties, and Performance. IEEE Transactions on Signal Processing, 2011, 59, 3576-3591.	5.3	193
382	Bistatic sar data focusing using an analytical spectrum based frequency scaling algorithm in tandem configuration. , 2011, , .		1
383	Space-surface bistatic SAR-GMTI. , 2011, , .		2
384	Two-dimensional spectrum for MEO SAR processing using a modified advanced hyperbolic range equation. Electronics Letters, 2011, 47, 1043.	1.0	19
385	低é‡é¢'采æ·SAR 系统ä,地é¢è¿åЍç>®æ‡å;æ•°ä¼°è®;. Scientia Sinica Informationis, 2011, 41, 1517-1528.	0.4	1
386	ISAR Imaging of High Speed Targets Based on LMSF Signal. Dianzi Yu Xinxi Xuebao/Journal of Electronics and Information Technology, 2011, 30, 2813-2817.	0.1	5
387	The Clutter Suppression Method of Airborne Multi-channel SAR-GMTI System. Dianzi Yu Xinxi Xuebao/Journal of Electronics and Information Technology, 2011, 30, 2831-2834.	0.1	5
388	A Chirp-Z Transform Imaging Algorithm for Missile-borne SAR with Diving Maneuver Based on the Method of Series Reversion. Dianzi Yu Xinxi Xuebao/Journal of Electronics and Information Technology, 2011, 32, 2861-2867.	0.1	10
389	Study on Sparse Aperture of Inverse Synthetic Aperture Imaging Ladar with Low SNR. Dianzi Yu Xinxi Xuebao/Journal of Electronics and Information Technology, 2011, 32, 2808-2813.	0.1	1
390	Bistatic SAR Data Focusing Using a Frequency Scaling Algorithm Based on an Analytical Spectrum in Tandem Configuration. Dianzi Yu Xinxi Xuebao/Journal of Electronics and Information Technology, 2011, 33, 1447-1452.	0.1	0
391	Spaceborne/Airborne Hybrid Sliding Spotlight Bistatic SAR Range-Doppler Imaging Algorithm. Dianzi Yu Xinxi Xuebao/Journal of Electronics and Information Technology, 2011, 33, 1851-1857.	0.1	0
392	Weighted Minimum Entropy Autofocus Algorithm for ISAR Imaging. Dianzi Yu Xinxi Xuebao/Journal of Electronics and Information Technology, 2011, 33, 1809-1815.	0.1	6
393	基于稀ç−çº;性è°f频æ¥èį›äį¡å•çš"ISAR æˆåf• Scientia Sinica Informationis, 2011, 41, 1529-1540.	0.4	0
394	Time-frequency characteristics based motion estimation and imaging for high speed spinning targets via narrowband waveforms. Science China Information Sciences, 2010, 53, 1628-1640.	4.3	15
395	Resolution Enhancement for Inversed Synthetic Aperture Radar Imaging Under Low SNR via Improved Compressive Sensing. IEEE Transactions on Geoscience and Remote Sensing, 2010, 48, 3824-3838.	6.3	271
396	Minimum Entropy via Subspace for ISAR Autofocus. IEEE Geoscience and Remote Sensing Letters, 2010, 7, 205-209.	3.1	52

#	Article	IF	CITATIONS
397	Scaling the 3-D Image of Spinning Space Debris via Bistatic Inverse Synthetic Aperture Radar. IEEE Geoscience and Remote Sensing Letters, 2010, 7, 430-434.	3.1	42
398	Motion Parameter Estimation in the SAR System With Low PRF Sampling. IEEE Geoscience and Remote Sensing Letters, 2010, 7, 450-454.	3.1	39
399	Single-Range Image Fusion for Spinning Space Debris Radar Imaging. IEEE Geoscience and Remote Sensing Letters, 2010, 7, 626-630.	3.1	12
400	ISAR Imaging of Maneuvering Targets Based on the Range Centroid Doppler Technique. IEEE Transactions on Image Processing, 2010, 19, 141-153.	9.8	79
401	Adaptive two-step calibration for high-resolution and wide-swath SAR imaging. IET Radar, Sonar and Navigation, 2010, 4, 548.	1.8	58
402	Subimage fusion for high-resolution ISAR imaging. , 2010, , .		2
403	SAR imaging and Doppler ambiguity removal with distributed microsatellite arrays. International Journal of Remote Sensing, 2010, 31, 6441-6458.	2.9	2
404	A New Method of High Resolution ISAR Imaging under Low SNR Based on Improved Compressive Sensing. Dianzi Yu Xinxi Xuebao/Journal of Electronics and Information Technology, 2010, 32, 2263-2267.	0.1	2
405	Two-Dimensional Spectrum Matched Filter Banks for High-Speed Spinning-Target Three-Dimensional ISAR Imaging. IEEE Geoscience and Remote Sensing Letters, 2009, 6, 368-372.	3.1	12
406	Achieving Higher Resolution ISAR Imaging With Limited Pulses via Compressed Sampling. IEEE Geoscience and Remote Sensing Letters, 2009, 6, 567-571.	3.1	225
407	Experimenttation system of synthetic aperture imaging lidar. Journal of Electronics, 2009, 26, 433-437.	0.2	1
408	Research on indoor experimentation of range SAL imaging system. Science in China Series D: Earth Sciences, 2009, 52, 3098-3104.	0.9	7
409	Unparallel trajectory bistatic spotlight SAR imaging. Science in China Series F: Information Sciences, 2009, 52, 91-99.	1.1	4
410	Detection, parameter estimation and imaging of maneuvering target in wide-band signal. Science in China Series F: Information Sciences, 2009, 52, 1015-1026.	1.1	3
411	High-speed ground moving target detection research using triangular modulation FMCW. Frontiers of Electrical and Electronic Engineering in China: Selected Publications From Chinese Universities, 2009, 4, 127-133.	0.6	9
412	Keystone transformation of the Wigner–Ville distribution for analysis of multicomponent LFM signals. Signal Processing, 2009, 89, 791-806.	3.7	66
413	Motion Compensation for UAV SAR Based on Raw Radar Data. IEEE Transactions on Geoscience and Remote Sensing, 2009, 47, 2870-2883.	6.3	219
414	Narrow-Band Interference Suppression for SAR Based on Complex Empirical Mode Decomposition. IEEE Geoscience and Remote Sensing Letters, 2009, 6, 423-427.	3.1	89

#	Article	IF	CITATIONS
415	Coherence-Improving Algorithm for Image Pairs of Bistatic SARs With Nonparallel Trajectories. IEEE Transactions on Geoscience and Remote Sensing, 2009, 47, 2884-2898.	6.3	5
416	High-Resolution Three-Dimensional Imaging of Spinning Space Debris. IEEE Transactions on Geoscience and Remote Sensing, 2009, 47, 2352-2362.	6.3	71
417	Application of compressed sensing in sparse aperture imaging of radar. , 2009, , .		12
418	Micro-Doppler analysis and imaging of air-planes with rotating parts. , 2009, , .		6
419	A Matched-Filter-Bank-Based 3-D Imaging Algorithm for Rapidly Spinning Targets. IEEE Transactions on Geoscience and Remote Sensing, 2009, 47, 2106-2113.	6.3	23
420	Unambiguous Reconstruction and High-Resolution Imaging for Multiple-Channel SAR and Airborne Experiment Results. IEEE Geoscience and Remote Sensing Letters, 2009, 6, 102-106.	3.1	25
421	Chirp scaling algorithm for parallel bistatic SAR data processing. , 2009, , .		2
422	High-Resolution Three-Dimensional Radar Imaging for Rapidly Spinning Targets. IEEE Transactions on Geoscience and Remote Sensing, 2008, 46, 22-30.	6.3	86
423	Bistatic Spotlight SAR Processing Using the Frequency-Scaling Algorithm. IEEE Geoscience and Remote Sensing Letters, 2008, 5, 48-52.	3.1	79
424	The Polar Format Imaging Algorithm Based on Double Chirp-Z Transforms. IEEE Geoscience and Remote Sensing Letters, 2008, 5, 610-614.	3.1	40
425	Imaging of Micromotion Targets With Rotating Parts Based on Empirical-Mode Decomposition. IEEE Transactions on Geoscience and Remote Sensing, 2008, 46, 3514-3523.	6.3	134
426	A New Look at the Bistatic-to-Monostatic Conversion for Tandem SAR Image Formation. IEEE Geoscience and Remote Sensing Letters, 2008, 5, 392-395.	3.1	16
427	A method for multiple ship target imaging based on hybrid SAR/ISAR method. , 2008, , .		2
428	Parameters estimation of LFM signals based on STTFD. , 2008, , .		2
429	A Novel Modified Omega-K Algorithm for Synthetic Aperture Imaging Lidar through the Atmosphere. Sensors, 2008, 8, 3056-3066.	3.8	7
430	Focusing general bistatic SAR using analytically computed point target spectrum. , 2007, , .		2
431	Motion compensation technique for high resolution spotlight SAR. , 2007, , .		2
432	Raw data based azimuth ambiguities removing. , 2007, , .		1

#	Article	IF	CITATIONS
433	Modified phase history model for high resolution spaceborne bistatic SAR. , 2007, , .		0
434	Experimental reaserch of unsupervised Cameron/ML Classification method for fully polarimetric SAR Data. , 2007, , .		1
435	A novel approach to three-channel SAR-GMTI channel equalization and moving target detection and location based on real data. , 2007, , .		0
436	A new channel equalization method for airborne multi-channel SAR-GMTI system. , 2007, , .		0
437	SRMF-CLEAN Imaging Algorithm for Space Debris. IEEE Transactions on Antennas and Propagation, 2007, 55, 3524-3533.	5.1	67
438	Focusing Parallel Bistatic SAR Data Using the Analytic Transfer Function in the Wavenumber Domain. IEEE Transactions on Geoscience and Remote Sensing, 2007, 45, 3633-3645.	6.3	54
439	A New Algorithm for Sparse Aperture Interpolation. IEEE Geoscience and Remote Sensing Letters, 2007, 4, 480-484.	3.1	16
440	Single Range Matching Filtering for Space Debris Radar Imaging. IEEE Geoscience and Remote Sensing Letters, 2007, 4, 576-580.	3.1	21
441	Eigensubspace-Based Filtering With Application in Narrow-Band Interference Suppression for SAR. IEEE Geoscience and Remote Sensing Letters, 2007, 4, 75-79.	3.1	137
442	Suppression of Azimuth Ambiguities with Constellation of Micro-satellites. , 2006, , .		3
443	DBS imaging and GMTI in a wideband airborne mechanic scanning radar. Frontiers of Electrical and Electrionic Engineering in China: Selected Publications From Chinese Universities, 2006, 1, 410-415.	0.6	1
444	A New Algorithm for Sparse Aperture Extrapolation. , 2006, , .		0
445	An Effective Approach to Ground Moving Target Imaging for Single Channel SAR System. , 2006, , .		1
446	Radar HRRP target recognition based on higher order spectra. IEEE Transactions on Signal Processing, 2005, 53, 2359-2368.	5.3	189
447	Migration Through Resolution Cell Compensation in ISAR Imaging. IEEE Geoscience and Remote Sensing Letters, 2004, 1, 141-144.	3.1	158
448	<title>Doppler ambiguity resolving in sparse aperture SAR imaging</title> ., 2004, , .		0
449	Properties of high-resolution range profiles. Optical Engineering, 2002, 41, 493.	1.0	67
450	Logarithm bispectrum-based approach to radar range profile for automatic target recognition. Pattern Recognition, 2002, 35, 2643-2651.	8.1	23

#	Article	IF	CITATIONS
451	Time-frequency approaches to ISAR imaging of maneuvering targets and their limitations. IEEE Transactions on Aerospace and Electronic Systems, 2001, 37, 1091-1099.	4.7	81
452	Translational motion compensation and instantaneous imaging of ISAR maneuvering target. , 2001, , .		17
453	<title>Imaging algorithm for steadily flying and maneuvering big targets</title> . , 2001, , .		6
454	On the aspect sensitivity of high resolution range profiles and its reduction methods. , 0, , .		22
455	Principles and algorithms for inverse synthetic aperture radar imaging of manoeuvring targets. , 0, , .		5
456	One dimensional cross-range imaging and methods to improve the resolution of low resolution radar targets. , 0, , .		1
457	Imaging of maneuvering targets based on parameter estimation of multicomponent polynomial signals. , 0, , .		0
458	The properties of range profile of aircraft. , 0, , .		5
459	Correction of migration through resolution cell in ISAR imaging. , 0, , .		3
460	Radar target recognition by a logarithm bispectrum-based method. , 0, , .		1
461	ISAR echoes coherent processing and imaging. , 0, , .		10
462	Doppler ambiguity resolving in distributed micosatellites radar imaging [micosatellites read microsatellites]. , 0, , .		1
463	Adaptive Despeckling SAR Images Based on Scale Space Correlation. , 0, , .		0